ISSN 0027-1349, Moscow University Physics Bulletin, 2007, Vol. 62, No. 4, pp. 216–220. © Allerton Press, Inc., 2007.
Original Russian Text © T.G. Elizarova, P.N. Nikol'skii, 2007, published in Vestnik Moskovskogo Universiteta. Fizika, 2007, No. 4, pp. 14–17.

Numerical Simulation of the Laminar–Turbulent Transition in the Flow over a Backward-Facing Step

T. G. Elizarova[a] and P. N. Nikol'skii[b]

[a] *Institute for Mathematical Modeling, Russian Academy of Sciences, Miusskaya pl. 4a, Moscow, 125047 Russia*
e-mail: telizar@afrodita.phys.msu.ru

[b] *Department of Mathematics, Faculty of Physics, Moscow State University, Leninskie gory, Moscow, 119992 Russia*

Received June 7, 2006

Abstract—The capabilities of the quasi-gasdynamic equations as applied to the simulation of laminar–turbulent transitions are demonstrated by computing the viscous compressible gas flow in a channel with an abrupt expansion.

DOI: 10.3103/S0027134907040030

INTRODUCTION

Due to the development of computing machinery, direct numerical simulation based on the Euler or Navier–Stokes equations without using semiempirical turbulence models [1] is becoming a promising approach to the numerical study of turbulent flows. In this case, turbulent dissipation on subgrid scales is modeled by artificial regularizers. The dissipative mechanism of the regularizers plays the role of a filter that smoothes the subgrid fluctuations of gasdynamic variables. However, a detailed analysis of the dissipative characteristics of artificial regularizers used in nonlinear and nonstationary numerical models is a complicated mathematical problem, which is usually not considered on its own.

In this paper, the direct numerical simulation of turbulent viscous compressible gas flows is based for the first time on the quasi-gasdynamic (QGD) equations [2–4]. In contrast to the Navier–Stokes and Euler equations, they involve additional conservative terms resulting from the additional time smoothing of gasdynamic variables (density, velocity, and temperature). These additional terms play the role of regularizers and ensure the stability and accuracy of the numerical algorithms based on them. There is a theorem stating that the total thermodynamic entropy does not decrease for the QGD equations, which confirms the dissipative nature of the corresponding regularizers.

In [5], a numerical algorithm based on the QGD equations was developed for computing subsonic viscous gas flows. We use this algorithm to simulate the flow over a backward-facing step in a two-dimensional channel, in which case an increase in the Reynolds number is accompanied by the transition from laminar to turbulent flows. The numerical results are compared with the experimental data in [6], which are considered classic for this problem and are used to test numerical algorithms (see, e.g., [7, 8] and the bibliography therein). The flow behind the step in [6] can be treated as two-dimensional with reasonable accuracy.

STATEMENT OF THE PROBLEM AND NUMERICAL METHOD

In conventional notation, the QGD equations have the form

$$\frac{\partial \rho}{\partial t} + \operatorname{div}\mathbf{j}_m = 0, \tag{1}$$

$$\frac{\partial(\rho\mathbf{u})}{\partial t} + \operatorname{div}(\mathbf{j}_m \otimes \mathbf{u}) + \nabla p = \operatorname{div}\Pi, \tag{2}$$

$$\frac{\partial}{\partial t}\left[\rho\left(\frac{\mathbf{u}^2}{2} + \varepsilon\right)\right] + \operatorname{div}\left[\mathbf{j}_m\left(\frac{\mathbf{u}^2}{2} + \varepsilon + \frac{p}{\rho}\right)\right] + \operatorname{div}\mathbf{q} = \operatorname{div}(\Pi \cdot \mathbf{u}). \tag{3}$$

Here, the mass flow density vector, viscous stress tensor, and heat flux are given by

$$\mathbf{j}_m = \rho(\mathbf{u} - \mathbf{w}), \quad \mathbf{w} = \frac{\tau}{\rho}[\operatorname{div}(\rho\mathbf{u} \otimes \mathbf{u}) + \nabla p], \tag{4}$$

$$\Pi = \Pi_{\mathrm{NS}} + \tau\mathbf{u} \otimes [\rho(\mathbf{u} \cdot \nabla)\mathbf{u} + \nabla p] + \tau I[(\mathbf{u} \cdot \nabla)p + \gamma p \operatorname{div}\mathbf{u}], \tag{5}$$

$$\mathbf{q} = -\kappa\nabla T - \tau\rho\mathbf{u}\left[(\mathbf{u} \cdot \nabla)\varepsilon + p(\mathbf{u} \cdot \nabla)\left(\frac{1}{\rho}\right)\right], \tag{6}$$

Parameters and numerical results

Re	h	α	β	dt	L	L_s [6]	L_s	T_f
100*	0.05	0.5	0.2	0.0010	10	5.0	5.0	81
200*	0.05	0.5	0.2	0.0010	14	8.5	8.4	204
300	0.05	0.5	0.3	0.0015	20	11.3	10.4	300
400*	0.05	0.5	0.2	0.0010	20	14.2	12.7	626
600	0.05	0.3	0.5	0.0025	30	17.0	16.0	400
		0.5	0.3	0.0015			15.5	
700	0.05	0.3	0.5	0.0025	30	15.5	15.7	400
		0.5	0.3	0.0015			17.0	
1000	0.03	0.3	0.5	0.0015	30	13.8	10.6	400
		0.5	0.3	0.0009			11.4	
2000	0.05	0.3	0.5	0.0025	30	9.0	9.1	400
		0.5	0.3	0.0015			10.9	
2800	0.05	0.3	0.5	0.0025	30	6.1	7.2	400
		0.5	0.3	0.0015			8.8	
3500	0.05	0.3	0.5	0.0025	30	8.0	7.8	400
		0.5	0.3	0.0015			9.0	

Note: The star denotes the data of [5].

where Π_{NS} is the Navier–Stokes viscous stress tensor and τ is a parameter of temporal smoothing that has the dimension of time and is defined as

$$\tau = \frac{\eta}{p\mathrm{Sc}} + \alpha\frac{h}{c}. \quad (7)$$

Here, $\eta = \eta_0(T/T_0)^\omega$ is the dynamic viscosity, Sc is the Schmidt number, h is the minimal resolved length scale (the mesh size in this problem), $c = \sqrt{\gamma RT}$ is the speed of sound, $0 < \alpha < 1$ is a numerical coefficient, and h/c is the time required for a perturbation to travel across a grid cell.

We consider the two-dimensional viscous gas flow over a backward-facing step of height H in a channel of length L and height $2H$. The Poiseuille profile with a section-averaged velocity U_0 is specified at the entrance section. The flow is characterized by the Reynolds and Mach numbers

$$\mathrm{Re} = \frac{\rho_0 U_0 H}{\eta_0}, \quad \mathrm{Ma} = \frac{U_0}{c_0}, \quad (8)$$

where ρ_0 and T_0 are the gas density and temperature at the entrance section of the channel. The channel walls are assumed to be adiabatic with the no-slip and impermeability conditions set for the velocity and with the downstream condition specified at the channel exit. The Poiseuille flow is used as the initial condition. The numerical algorithm is based on an explicit second-order accurate scheme used for all spatial derivatives. A detailed description of the algorithm can be found in [5].

A uniform mesh in both directions was used in the computations. The time step was determined by the stability condition $dt = \beta h/c$, where the coefficient $0 < \beta < 1$ was chosen in the course of computations.

NUMERICAL RESULTS

The computations were performed for a subsonic airflow at normal pressure with the molecular parameters $\gamma = 1.4$, $\mathrm{Pr} = 0.737$, $\omega = 0.74$, and $\mathrm{Sc} = 0.746$.

The basic numerical characteristics at $\mathrm{Ma} = 0.1$ are listed in the table. Here, L is the length of the computational domain and T_f is the dimensionless time at which the computations were completed. Figure 1 compares the computed length L_s of the separation zone with experimental data [6]. According to [6], the separation zone increases nearly linearly with the Reynolds num-

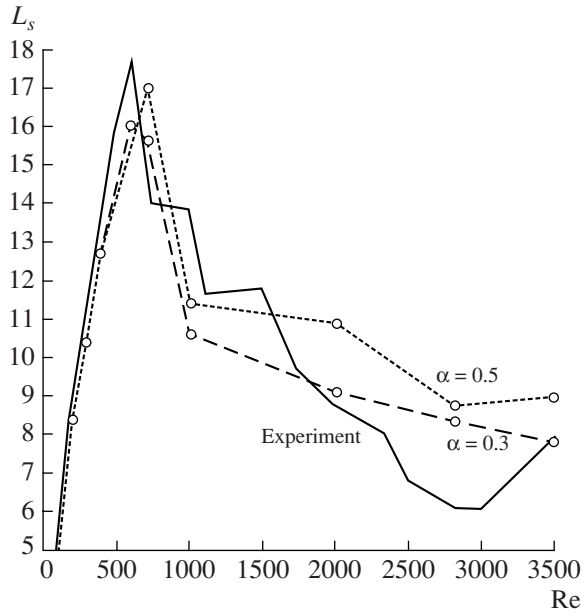

Fig. 1. Computed length of the separation zone (broken curves, the computed values are denoted by labels) as compared with the experimental data of [5] (solid curve).

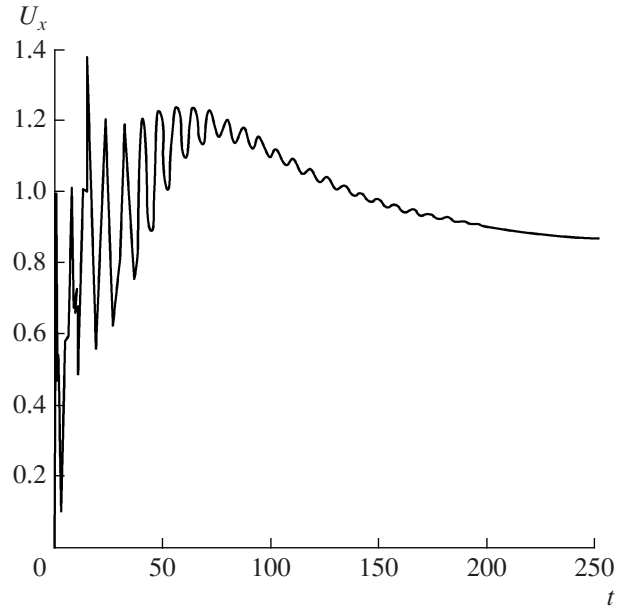

Fig. 2. Temporal evolution of the velocity at Re = 300.

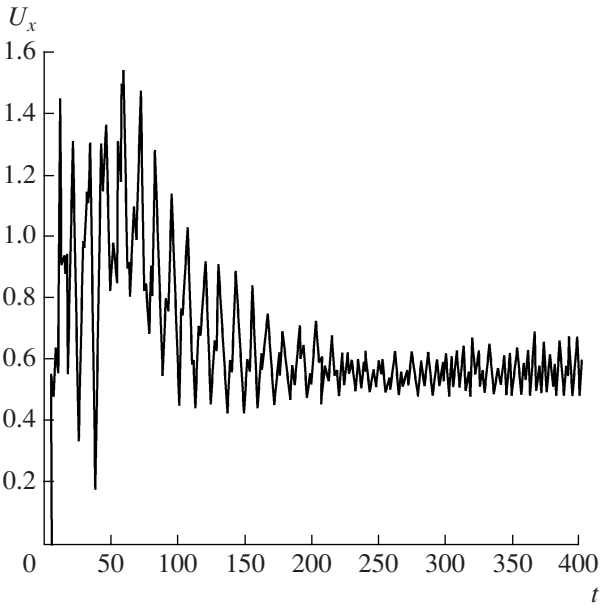

Fig. 3. Temporal evolution of the velocity at Re = 600.

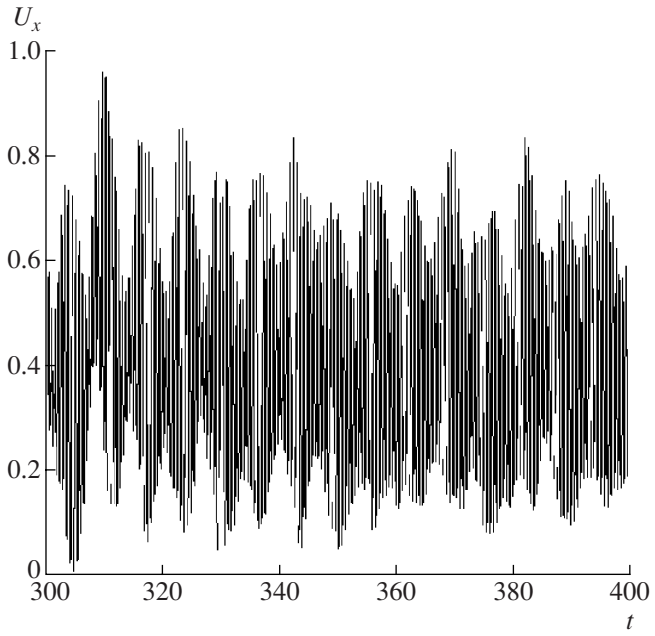

Fig. 4. Fragment of the temporal evolution of the velocity at Re = 1000.

ber[1] up to $Re_D = 1200$ and then decreases in the range $1200 < Re_D < 6600$. The decrease in the separation zone is associated with the unsteady flow developing behind the step.

For laminar flows (Re < 600), the recirculation flow behind the step is steady and the length of the separation zone agrees well with the experimental data and previous computations. For Re > 600, oscillations arise in the flow field and it becomes unsteady and turbulent. In this case, the length of the separation zone is determined from the averaged field. It can be seen that the separation zone decreases with increasing Re and the computed results agree fairly well with the experimental data. Note that the nonmonotonic decrease in L_s in the experiment can be explained by three-dimensional

[1] In [6] the Reynolds number was computed by formula (8), where the step height H was replaced by $D = 2H$.

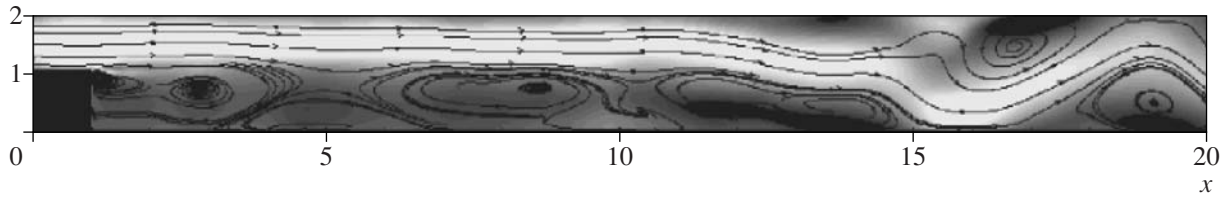

Fig. 5. Instantaneous streamlines at Re = 1000 (fragment).

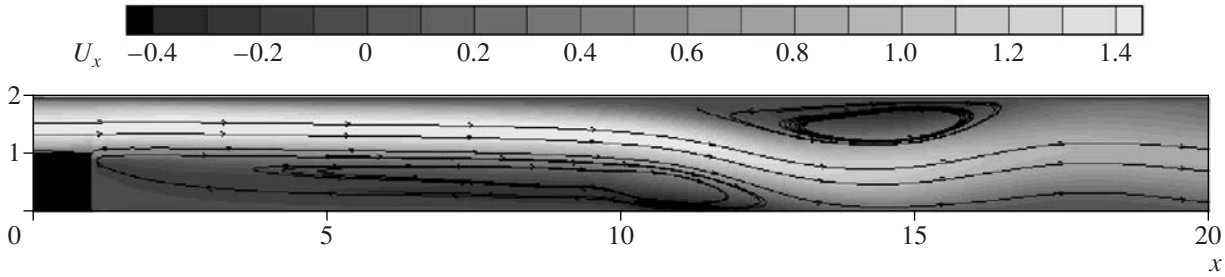

Fig. 6. Streamlines of the averaged flow at Re = 1000 (fragment).

vortex structures developing in the flow, which cannot appear in our numerical computations. According to numerous experimental data and numerical results (see [7, 8] and the references therein), the length of the separation zone nearly does not change at Re > 4000 and is $5 < L_s < 8$ depending on the geometry of the problem. For example, according to [8], $L_s = 5.5$ at Re = 3700.

Figures 2 and 3 show the temporal evolution of the longitudinal velocity at the point with coordinates (8, 1) for Re = 300 and Re = 600, respectively. The laminar flow at Re = 300 reaches a steady state. A transition regime with the appearance of velocity oscillations is observed at Re = 600. Figure 4 displays a fragment of the temporal evolution of the horizontal velocity for a turbulent flow (Re = 1000). In this case, the flow is basically unsteady. The length of the separation zone is determined after averaging the velocity field over time intervals in the range $300 < \Delta t < 400$. The averaged flow depends little on the averaging interval for $\Delta t > 5$. Figures 5 and 6 show the instantaneous and averaged flow patterns at Re = 1000. They agree qualitatively with the results of [8] obtained for Re = 3700.

In contrast to the experiment in [6], where the Mach number was about 0.001, we used Ma = 0.1. However, the compressibility effects are $O(\mathrm{Ma}^2)$ and their influence on the separation zone length can be regarded as insignificant. For laminar flows, this hypothesis is supported by the results of [5]. It was also shown in [5] that the length of the separation zone depends weakly on the mesh size h. For turbulent flows, the numerical experiments revealed that L_s also depends weakly on h for $h < 0.1$.

The formula for τ (see (7)) involves a free parameter, namely, the numerical coefficient $0 < \alpha < 1$. According to previous numerical experiments [3, 5, 9] and the present results, the length of the separation zone depends slightly on α for laminar flows but depends noticeably on it for turbulent flows. It can be expected that the effect of α on the averaged flow reduces with decreasing mesh size, since a progressively larger portion of the power spectrum and vortex structures is resolved by the grid [1].

In [9], similar results for the separation zone length in laminar and turbulent viscous incompressible flows over a backward-facing step were obtained in the framework of quasi-hydrodynamic equations.

In summary, we have demonstrated that the QGD algorithm can be used for direct numerical simulation of the laminar–turbulent transition in the flow over a backward-facing step. In contrast to other methods based on numerical models for computing laminar and turbulent flows (see, e.g., [1, 6–8]), the QGD algorithm offers a unified approach to the computation of both flow types and produces the transition from laminar to turbulent flows at Reynolds numbers corresponding to experimental data.

Despite the limitations of the two-dimensional spatial model, the numerical results agree well with experimental data. The numerical algorithm can be naturally extended to three dimensions and can be effectively implemented on multiprocessor computers, which would make it possible to simulate three-dimensional turbulent flows in the future.

REFERENCES

1. O. M. Belotserkovskii and A. M. Oparin, *Numerical Experiment in Turbulence: From Order to Chaos* (Nauka, Moscow, 2001) [in Russian].
2. Yu. V. Sheretov, *Mathematical Modeling of Fluid Flows Based on Quasi-Hydrodynamic and Quasi-Gasdynamic Equations* (Tversk. Gos. Univ., Tver, 2000) [in Russian].
3. T. G. Elizarova, M. E. Sokolova, and Yu. V. Sheretov, Zh. Vychisl. Mat. Mat. Fiz. **45**, 545 (2005) [Comput. Math. Math. Phys. **45**, 524 (2005)].
4. T. G. Elizarova, *Quasi-Gasdynamic Equations and Methods for Computing Viscous Flows* (Nauchnyi Mir, Moscow, 2007) [in Russian].
5. T. G. Elizarova and M. E. Sokolova, Vestn. Mosk. Univ., Fiz. Astron., No. 3, 6 (2005).
6. B. F. Armaly, F. Durst, J. C. F. Pereira, and B. Schonung, J. Fluid Mech. **127**, 473 (1983).
7. H. Le, P. Moin, and J. Kim, J. Fluid Mech. **330**, 349 (1997).
8. D. Wee, Yi. Tongxun, A. Annaswamy, and A. Ghoniem, Phys. Fluids **16**, 3361 (2004).
9. T. G. Elizarova, I. S. Kalachinskaya, Yu. V. Sheretov, and E. V. Shil'nikov, in *Applied Issues and Computer Science*, Ed. by D. P. Kostomarov and V. I. Dmitriev, (Maks Press, Moscow, 2003), No. 14, p. 85 [in Russian].